First Online: 25 January 2018 A. Yasin Alibhai

Swept Source Optical Coherence Tomography: a Review

Introduction

Optical coherence tomography (OCT) is a non-invasive imaging technique that enables in vivo imaging of biological tissue in cross-section [1]. Founded on the principles of low coherence interferometry, OCT creates images of anatomical structures based on back-reflected light, similar to the way reflections of ultrasonic waves are used to create an ultrasound image. Due to the optical properties of the eye, OCT is ideally suited for imaging of intraocular structures. During the past two decades, OCT has made a profound impact as a diagnostic tool in the field of ophthalmology.

Improvements made over time in sensitivity, acquisition speed, and resolution have enabled volumetric imaging of ocular structures to be

performed with micrometer-scale depth resolution [2]. With the advent of faster and higher resolution instrumentation, the capabilities of OCT have continued to evolve and improve. Clinicians have increasingly relied on OCT to qualitatively and quantitatively analyze anatomical alterations as a result of retinal, choroidal, optic nerve, and anterior segment diseases.

In this review of swept source OCT (SS-OCT), we shall attempt to explain the physics behind SS-OCT, the advantages and disadvantages of SS-OCT when compared with SD-OCT, and the current clinical applications of SS-OCT.

Commercial Advances in OCT

Introduced in 1991, the original OCT prototype used time-domain technology (TD-OCT) and employed a moving reference arm [1, 3, 4, 5]. Early commercial OCT devices had limited resolution and were burdensome to use. In 2002, Carl Zeiss Meditec commercialized the Stratus OCT device, which was easier to use and offered much improved quality of images, and OCT became much more widely used in the

third-generation TD-OCT device only allowed scanning speeds of up to 400 A-scans per second. Although the axial resolution could be improved with more advanced light sources, the time to acquire these ultrahigh-resolution TD-OCT images was burdensome, and most TD-OCT devices therefore offered a limited axial resolution of ~ 10 μm [6]. Although the images were clinically useful, the speed limitations of TD-OCT limited its clinical utility and overall uptake.

Hardware advancements and technical developments in the field allowed OCT instruments to use Fourier-domain detection methods, enabling exponentially faster scanning speeds, and improved resolution compared to TD-OCT. The increase in imaging speed allowed for much higher pixel density, improving image quality, and greater retinal coverage, enabling three-dimensional OCT imaging and accurate image registration to the fundus. With the development of fourier domain OCT (FD-OCT), a new wave of commercial OCT instruments exploded into the market. The first FDA-approved fourier domain OCT device became available in 2006.

produced commercially available spectral domain OCT instruments. The use of these OCT instruments in the clinic has increased dramatically, and OCT has now become a critical assessment device in most eye clinics.

Fourier Domain OCT (Spectral Domain Versus Swept Source OCT)

Fourier domain OCT (FD-OCT) does not employ a moving reference arm and works by measuring the interfered light in the so-called "Fourier domain" [7, 8, 9, 10, 11, 12, 13]. A mathematical operation, called the Fourier transformation, converts measurements of interfered light into physical delays or distances. FD-OCT is able to measure all of the light from different delays, achieving axial resolutions nearing 2 μm (with advanced light sources), and image acquisition speeds of between 26,000 and 100,000 A-scans/s in current commercially available devices, or up to 1,700,000 A-scans/s in advanced FD-OCT prototypes [14, 15]. There are two commonly used applications of FD-OCT: spectral-domain OCT (SD-OCT) [7, 8, 9, 10] and swept-source OCT (SS-OCT) [11, 12, 13].

SD-OCT uses a continuous light source (super luminescent diode laser), that emits a broad range of wavelengths. Detection of the back scattered light is done by separating the interfered light into its different wavelength components using a spectrometer and a line scan camera, a one-dimensional array of detectors which is digitally read at high speed. The A-scan rate is determined by the exposure and read-time of the line scan camera (how long it takes to digitally read the camera's pixel values).

In contrast, SS-OCT uses a tunable swept laser as its light source. This emits, at any instant in time, a "single" wavelength, and sweeps across a broad range of wavelengths as a function of time. The interference spectrum is detected by a single photodetector whose output is digitized as the wavelength is swept. Unlike SD-OCT, the A-scan rate of SS-OCT is set by the rate at which the light source is swept.

Advantages of Swept Source OCT

Currently available commercial SD-OCT systems typically employ an 800- to 900-nm

ranging from 40 to 100 kHz [16]. SS-OCT devices typically use wavelengths above 1000 nm and operate at speeds equal to or greater than 100 kHz [17]. The shorter wavelengths utilized in most SD-OCT devices undergo relatively more scattering and attenuation, especially from tissue containing melanin. Consequently, SD-OCT suffers from signal decay with increasing tissue depth and offers limited visualization of structures beyond the RPE [18•, 19]. Therefore, SS-OCT offers potential advantages in visualization of the choroid and sclera (Fig. 1).

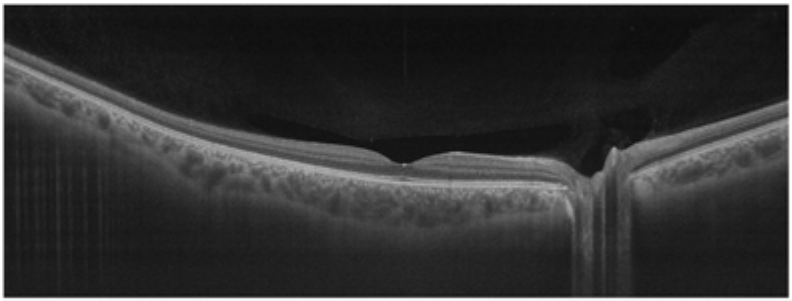

Fig. 1

OCT B scan of a normal eye imaged using SS-OCT. The B scan is 16 mm in length and offers, within a single frame, clear visualization of the vitreous, retina, choroid, and sclera

In addition, the method of SD-OCT acquisition results in signal roll-off at the fringes of the imaging spectrum, as all of the wavelengths of light are detected at once by the CCD camera. Conversely, the use of a swept source laser in SS-OCT allows the camera to detect a single wavelength at a time, which means there is no signal roll-off. Therefore, SS-OCT offers the potential for improved depth and range of imaging, allowing for simultaneous viewing of different ocular structures without movement of the OCT focus or utilization of enhanced depth OCT [20, 21].

Imaging speeds of SS-OCT are also easier to increase compared to SD-OCT, as the development of the complex CCD cameras necessary for SD-OCT has been more costly and difficult to use in prototype instruments. Improved imaging speeds offered with SS-OCT allow for improvements in widefield, three-dimensional, and real-time OCT imaging in the clinic as well as in the operating suite [22].

Limitations of Swept Source OCT

However, longer wavelengths are more readily

comprises mostly water, this places a limit on the use of longer wavelengths in SS-OCT imaging of the eye [13]. The necessity to use longer wavelengths in SS-OCT also means that SS-OCT offers a slightly reduced image resolution relative to SD-OCT [17]. This is because axial resolution in OCT imaging is directly proportional to the bandwidth of the light source used. SS-OCT is limited by the bandwidth that can be used when light absorption by water is factored in.

The overall uptake of SS-OCT remains limited, as the cost of development has proven to be prohibitive. Additionally, the clinical significance of enhanced visualization of the choroid and increased depth of imaging remains to be determined. As a result, manufacturers remain skeptical when it comes to allocating more resources towards further development of this technology. This is reflected in the limited availability of commercial SS-OCT instruments. As of writing this review, there is only one commercially available ophthalmic SS-OCT device. The Triton™ SS-OCT (Topcon, Tokyo, Japan) is currently available for sale in several countries

centered at 1050 nm with an A scan rate of 100 kHz. The PlexElite™ (Carl Zeiss Meditec, Dublin, California) is currently available for investigational purposes only and similarly uses a central wavelength of 1050 nm with an A scan rate of 100 kHz.

The Massachusetts Institute of Technology (MIT) has built a research prototype that uses a vertical cavity surface emitting laser (VCSEL) centered at 1060 nm with an A scan rate of 400 kHz [23]. This ultrahigh-speed SS-OCT is capable of measuring the velocity of blood in the central retinal arteries and has been used in several clinical studies [24, 25]. Additionally, faster prototype devices have been developed with the fastest A-scan rate being reported at 1.68 mHz by Huber's group in Germany [15]. Despite the improvements in speed, it remains to be seen whether SS-OCT enters into mainstream clinical ophthalmology or continues to be merely a research tool.

Clinical Applications

Choroido-Scleral Imaging

Despite SD-OCT and the enhanced depth imaging (EDI) technique, which offers improvements in the quality of choroidal visualization, the introduction of SS-OCT has enabled more consistent and higher quality images of the choroid [21, 26]. SS-OCT imaging has allowed clinicians and researchers to individually visualize and correlate with known histology the layers of the choroidal vasculature (choriocapillaris, Sattler's layer, and Haller's layer), which were previously not distinguishable using conventional SD-OCT [27]. Additionally, SS-OCT is better able to separate the choroidal-scleral junction including the supra-choroidal space [28].

Previously, measurements of choroidal thickness were being performed using SD-OCT and EDI at either a single point under the fovea or at several predetermined retinal positions. Using SS-OCT, choroidal thickness has been measured in healthy eyes, with results contradicting those from studies that used SD-OCT [29, 30]. While these differences in measurements can be attributed to several factors, the improved visualization of ocular layers with SS-OCT is a likely contributor

Open image in new window

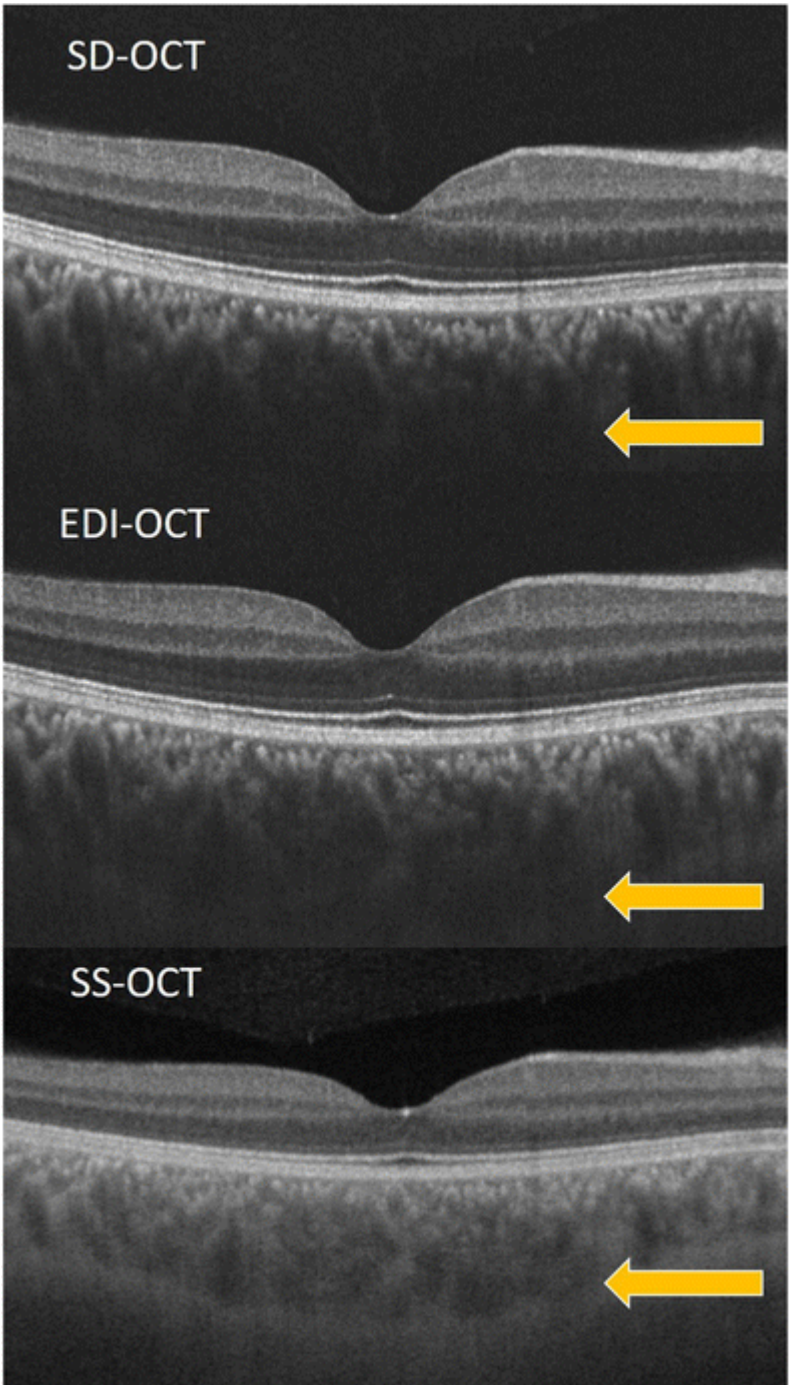

Fig. 2

OCT B scan of the same eye imaged using SD-OCT, EDI-OCT, and SS-OCT. Note the increased OCT signal penetration and resulting improvement in visualization of the choroid and choroido-scleral junction (yellow arrows)

Denser scanning patterns have enabled three-dimensional topographic maps to be generated, covering large areas of the posterior pole (Fig. 3). These have helped in studying the choroid in healthy eyes, AMD, and diabetic retinopathy [31, 32, 33]. The topographic variance of choroidal thickness over the posterior pole has been observed using these thickness maps with studies showing localized and focal thickening or thinning with different disease processes. Changes in choroidal layer thickness following vitrectomy and ILM peeling have also been observed using SS-OCT [34].

[Open image in new window]

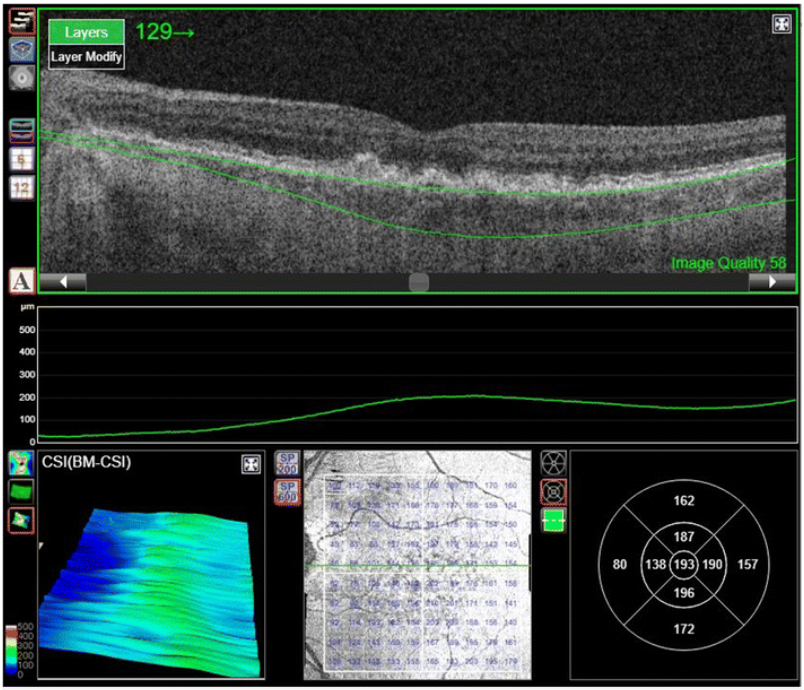

Fig. 3

An automated choroidal thickness map from a patient with intermediate AMD generated using the Triton™ SS-OCT. Maps such as these allow clinicians and researchers to study, and longitudinally follow up, the choroid in health and disease

SS-OCT has allowed more detailed in vivo qualitative analysis to be made for known chorio-retinal pathology. For example, SS-OCT has shown areas of varying reflectivity within

histopathology [35]. Choriocapillaris alterations are more clearly visualized under drusen using SS-OCT as compared to SD-OCT [36]. An observational case series of choroidal tumors demonstrated that SS-OCT was able to provide views of the tumor's internal structures along with accurate measurements of tumor diameter in every case [37]. Furthermore, a case series studying the anatomic characteristics of peripapillary intrachoroidal cavitation was able to demonstrate, with SS-OCT imaging, that cavities of the choroid can occur without causing deformities in either the retina or RPE because of posterior scleral bowing [38].

En-face SS-OCT imaging has helped in our understanding various disease processes. Findings of studies on the pachychoroid spectrum disorder include choroidal thickening, dilated choroidal vessels at the level of choriocapillaris, and possible visualization of choroidal neovascular membranes [39, 40]. In polypoidal choroidal vasculopathy (PCV), en-face SS-OCT imaging has shown vascular abnormalities to be present within the choroid. Additionally, it has

pigment epithelial detachments (RPEDs), irrespective of size, exist with PCV lesions which have been previously identified on indocyanine green angiography (ICGA) [41]. These studies have demonstrated additional features, often with important clinical correlations, that were not adequately demonstrable using SD-OCT.

Improved visualization of the sclera using SS-OCT has also allowed researchers to gain insight into alterations of scleral vasculature, seen in conditions such as pathologic myopia [42]. In a direct comparison between SS-OCT and SD-OCT imaging, SS-OCT was able to better visualize structures, such as the choroid, inner segment (IS)/outer segment (OS) line, and external limiting membrane (ELM) in patients with pathologic myopia [43]. Using SS-OCT to form 3-D reconstructions of dome-shaped maculas, Ellabban et al. described scleral thinning in RPE protrusions within the staphyloma. They also described uneven thinning of the sclera parafoveally, which was thought to induce the band-like ridge found between staphylomas [44]. Similarly, Ohsugi et al. demonstrated that a dome-shaped macula

sclera, which may lead to RPED formation, whereas thinning of the sclera owing to long-term changes and elongation of the axis may contribute to the development of CNV [45]. Morphologic changes in the choroid and sclera, including thickness variations, in peripapillary staphylomas have also recently been described using SS-OCT [46].

Vitreo-Retinal Imaging

Because of improved imaging depth and speed, SS-OCT is capable of capturing images of a larger region of the posterior vitreous and retina in comparison to SD-OCT (Fig. 4). SS-OCT has been used in qualitative and quantitative analysis of the retina, vitreous, and optic disc. Plaques and folds resulting from epiretinal membranes (ERM), along with defects in the retinal nerve fiber layer (RNFL), are more clearly visualized using SS-OCT when compared with SD-OCT [47]. Kikushima et al. investigated the dynamics of macular hole (MH) closure in gas-filled eyes after vitrectomy using SS-OCT. They found a distinct closure pattern and noted that MHs closing by day 1 had a significantly smaller minimum diameter

later. Additionally, confirmation of hole closure using SS-OCT allowed for the early discontinuation of face-down patient posturing [48].

Open image in new window

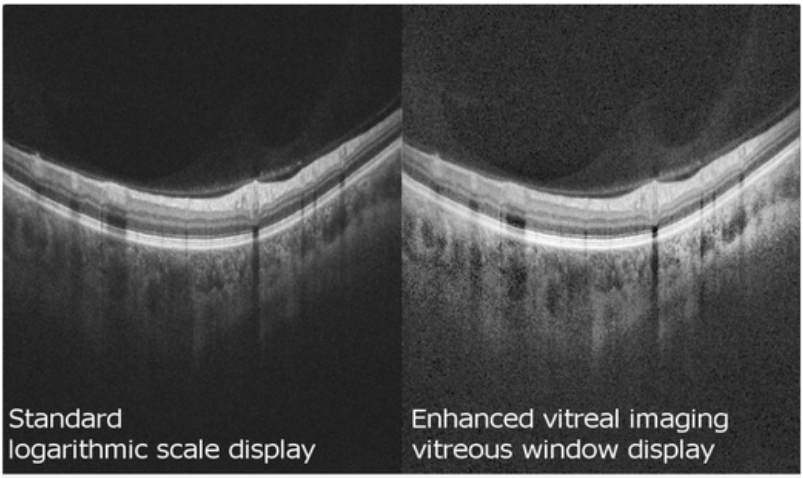

Fig. 4

Vitreoretinal Interface (VRI) and vitreous imaged with SS-OCT. SS-OCT allows for an enhanced visualization of the VRI and posterior vitreous. Additional details of the vitreous and VRI could be obtained using the vitreous window display (right panel) when compared to the standard logarithmic scale display (left panel)

Several studies have described the physiologic spaces and attachments of the vitreous in

focusing and window averaging SS-OCT, Spaide et al. described the normal anatomy of the posterior vitreous, including the premacular bursa, area of Martegiani and supramacular bursa [49]. In another study, SS-OCT was found to have a 91.9% sensitivity in detecting vitreous structures [50]. Associations between the size of the premacular bursa, also termed the posterior precortical vitreous pocket (PPVP), and myopic refractive errors have been described, along with studies in children indicating the formation of PPVP starting at the age of 3 with connections to Cloquet's canal starting at the age of 5, suggestive of a physiological role of the PPVP [51, 52]. Varying stages of vitreous degeneration, with structural defects such as prevascular vitreous fissures and posterior vitreous cisterns, have also been described using SS-OCT [53].

Optic Nerve Imaging

In a study of congenital optic disc pits and optic disc colobomas, SS-OCT was able to detect defects of the lamina cribosa (LC), different shapes of the cavities, and visualization of the

analysis of patients with tilted disc syndrome (TDS) by SS-OCT and 3D MRI suggests that the underlying cause is a deformity of the inferior globe below the optic nerve, and that the positional relationship between the fovea and inferior protrusion determines the degree of myopia [55]. A recent review of optic nerve head drusen (ONHD) and newer imaging modalities outlined the potential role of SS-OCT in longitudinally following up changes in drusen dimensions, and possibly improving our understanding of drusen-related visual field loss [56].

SS-OCT imaging in glaucoma has shown that patients with primary open-angle glaucoma have a more posteriorly located LC insertion, which may lead to the optic nerve excavation observed in glaucoma [57]. With comparison made between images taken with the adaptive optics-scanning light ophthalmoscope, Hood et al. have demonstrated that SS-OCT en-face images are able to detect small defects in the RNFL that were missed on the SD-OCT RNFL thickness maps, although others have suggested that SS-OCT's glaucoma diagnostic ability is similar to that of SD-OCT [58, 59]. LC

found to be independently correlated with cupping formation and tissue blood flow, with measurement of LC thickness being suggested as a method for the diagnosis and monitoring of glaucoma [60, 61]. Peripapillary choroidal thinning has also been noted in patients with open-angle glaucoma (POAG) but this has not been associated with glaucoma severity [62].

Anterior Segment Imaging

With SS-OCT's faster scanning speed, Mak et al. were able to perform 360° imaging of the iris and found that iris volume decreased not only in normal individuals and patients with primary POAG, but also in patients with angle closure after pupillary dilation [63]. Using a prototype 100-kHz SS-OCT system, Poddar et al. were able to post operatively study the 3-D morphology of the Boston KPro prosthesis, its position with respect to the surrounding tissue, and precisely evaluate success of the surgical procedure [64]. This was previously not possible with SD-OCT systems due to limited acquisition speed, resolution, and axial imaging range.

Until recently, OCT imaging could only identify structural changes in the macula as a result of chorio-retinal pathology. With the introduction of optical coherence tomography angiography (OCTA), underlying vascular changes can now be identified. OCTA is a noninvasive, dye-free OCT-based imaging technique that allows for volumetric visualization of vasculature. Multiple sequential OCT-B scans are acquired in rapid succession and then compared; the movement of blood cells from one image to the next creates a decorrelation signal which is then used to generate three-dimensional angiograms of retinal and choroidal vasculature. OCTA imaging can be performed using both SD-OCT and SS-OCT instruments, with both applications of FD-OCT conferring their strengths and weakness to the visualization of vasculature.

SS-OCTA imaging has several advantages when compared with SD-OCTA. The faster scanning speed of SS-OCTA allows for denser scan patterns and larger scan areas for a given acquisition time. SS-OCTA also suffers from less signal attenuation with increasing tissue

superior at visualizing structures below the RPE, including the choriocapillaris (CC). Several groups have reported that SS-OCTA was better at identifying type 1 CNV lesions based on improved visibility of the CNV's margins and lesion characteristics [18•, 19, 65] (Fig. 5). Another study has reported that SS-OCTA was able to identify type 1 CNV lesions that correspond to ICGA plaques in asymptomatic eyes of patients with intermediate age-related macular degeneration (AMD) [66].

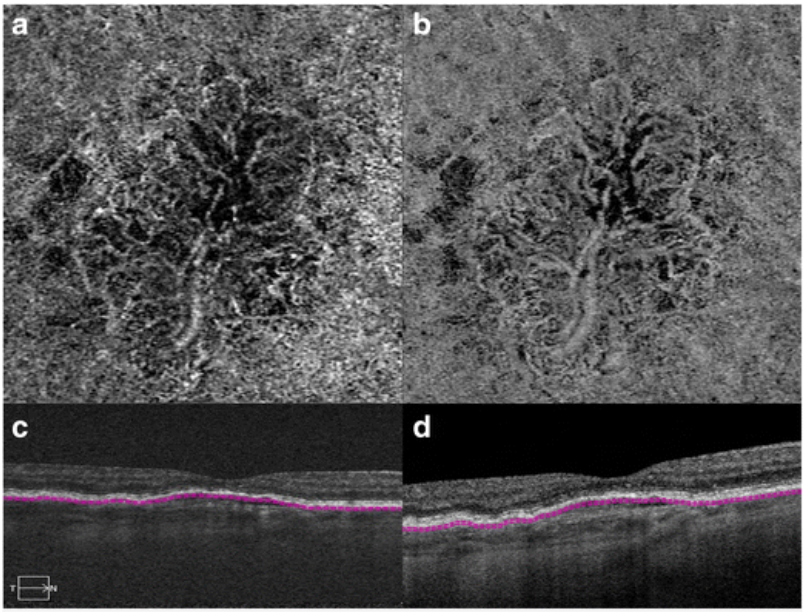

Fig. 5

OCTA of a CNV lesion secondary to exudative AMD imaged on the same day using SD-OCTA (Cirrus AngioPlex™) and SS-OCTA (PLEX™ Elite 9000). **a**, **c** Enface SD-OCTA and corresponding B-Scan of CNV lesion viewed using the manufacturers default choriocapillaris segmentation. **b**, **d** En-face SS-OCTA and corresponding B-Scan of CNV lesion viewed using the manufacturers default choriocapillaris segmentation. Both OCT instruments used employ the same software algorithm in order to generate the following OCTA. Subtle characteristics such as the branching pattern of the CNV lesion are more readily visualized using SS-OCTA

Faster scanning speeds also enable acquisition of multiple OCT volumes. By using variable interscan time analysis (VISTA), Fujimoto's group have demonstrated that SS-OCTA is capable of detecting regions of altered blood flow [67•, 68]. Areas previously showing low decorrelation flow signal will have an increased decorrelation signal. By using VISTA, they showed varying degrees of focal and diffuse CC alteration and flow impairment around regions of geographic atrophy, nascent geographic atrophy, and drusen-associated geographic

prove to be a valuable tool in helping our understanding of AMD pathogenesis.

Open image in new window

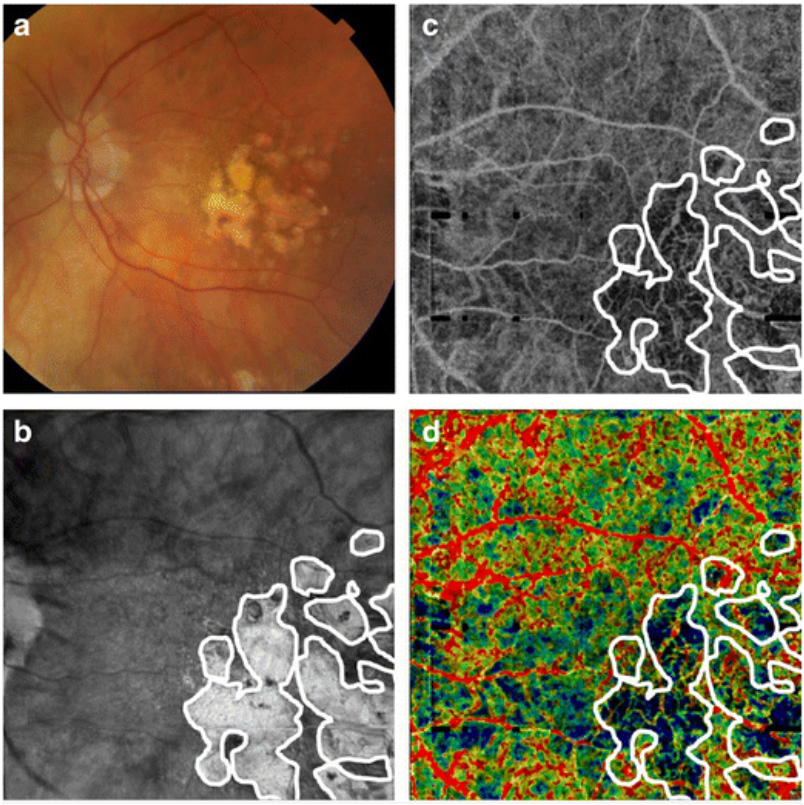

Fig. 6

Geographic atrophy (GA) imaged using a prototype 400-kHz VCSEL SS-OCT device. **a** Color fundus image showing areas of GA. **b** Corresponding SS-OCT fundus image with areas of GA highlighted using white borders. **c** Corresponding en-face OCTA image generated using variable interscan time analysis (VISTA). **d** Color-coded representation of VISTA showing

areas of altered choricapillaris blood flow around GA (Courtesy of Nadia K. Waheed, MD)

Intraoperative Swept Source OCT

Intraoperative OCT enables high-resolution visualization of intraocular details that cannot be visualized through the microscope alone. It may be useful in planning surgery, tracking surgical maneuvers, assessing outcomes, and potentially impacting surgical decision making. Recently, several groups have demonstrated prototype SS-OCT intraoperative systems. Carrasco-Zevallos et al. have been able to capture and render 3D-OCT data in real time, reporting on improvements in the performance of select depth-based maneuvers in mock surgical trials compared to maneuver guidance with the operating microscope alone [22]. Additionally, Chen et al. (unpublished) have been able to acquire widefield OCT images intraoperatively ($12 \times 12 mm^2$ for posterior segment and $10 \times 10 mm^2$ for anterior segment) in a very short period of time using their ultrahigh speed SS-OCT. 3-D volume rendering and widefield OCT imaging is only possible due

SS-OCT. Despite these benefits, further studies are needed to clarify the clinical utility of SS-OCT technology within the operating room.

Conclusion

SS-OCT is a variation of Fourier-Domain OCT that offers improvements in visualizing the vitreous, retina, choroid, and sclera. The increased scan speeds, decreased signal attenuation, and deeper tissue penetration make SS-OCT ideal for capturing wide fields of view and for studying structures below the RPE, especially the choroid. However, current acceptance of SS-OCT technology is limited by high costs of manufacturing and an unproven clinical benefit. Despite the current challenges, the overall simpler design of SS-OCT instruments should enable them to be produced in a more compact form and at lower costs in the future, making them a viable option for further commercial development.
